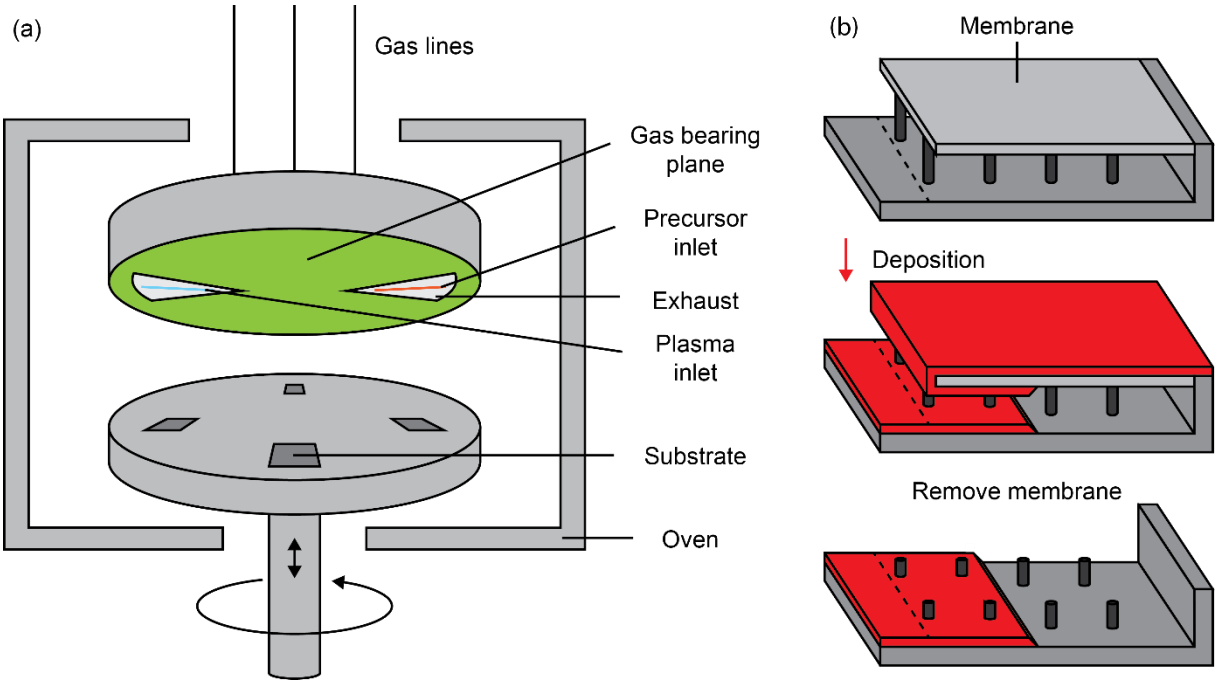

Figure 1: Schematic overview of experimental setup. (a) Rotary s-ALD reactor used to deposit TiO_2 films on planar substrates and PillarHall chips. (b) Cross-section of a lateral high-aspect-ratio structure present on the PillarHall chip. The dashed line indicates the start of the trench.

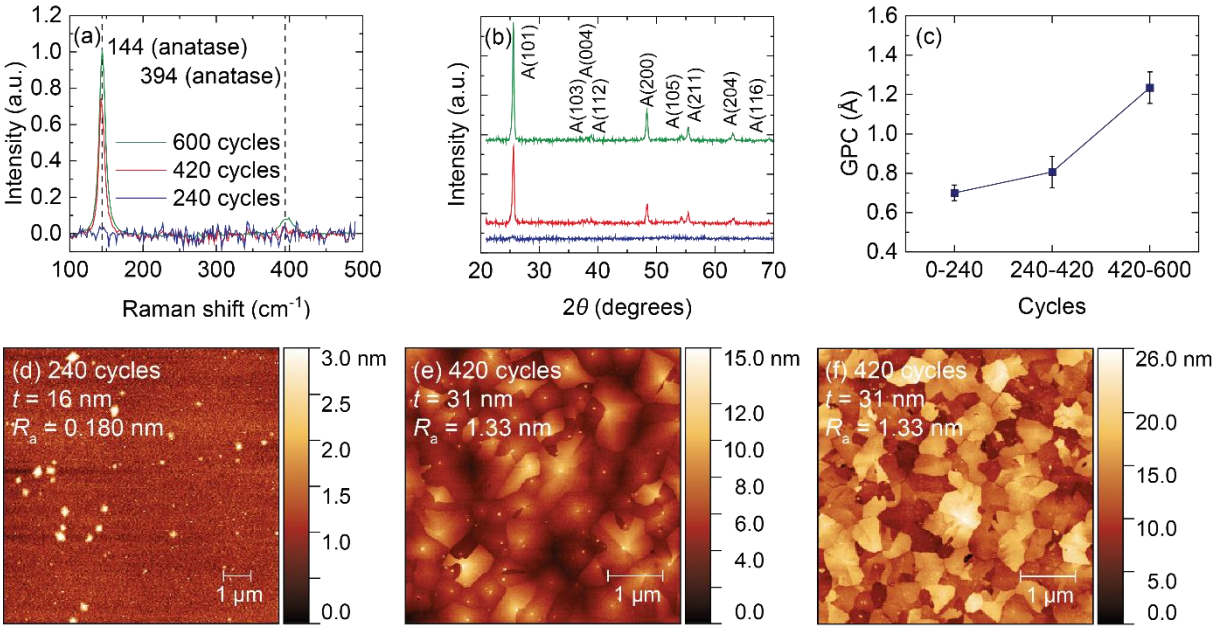

Figure 2: Amorphous-to-anatase-crystalline phase transition of TiO_2 deposited on a planar substrate is observed when increasing the number of cycles. The growth rate is enhanced by the anatase surface. (a) Raman spectra normalized for film thickness, with dashed lines indicating characteristic peak positions for anatase TiO_2, (b) grazing-incidence XRD diffractograms, (c) average GPC determined by spectroscopic ellipsometry measurements on three separate samples, and (d-f) AFM images of PE-s-ALD TiO_2 on planar Si substrates at deposition temperature of 200°C, for 240, 420, and 600 ALD cycles.

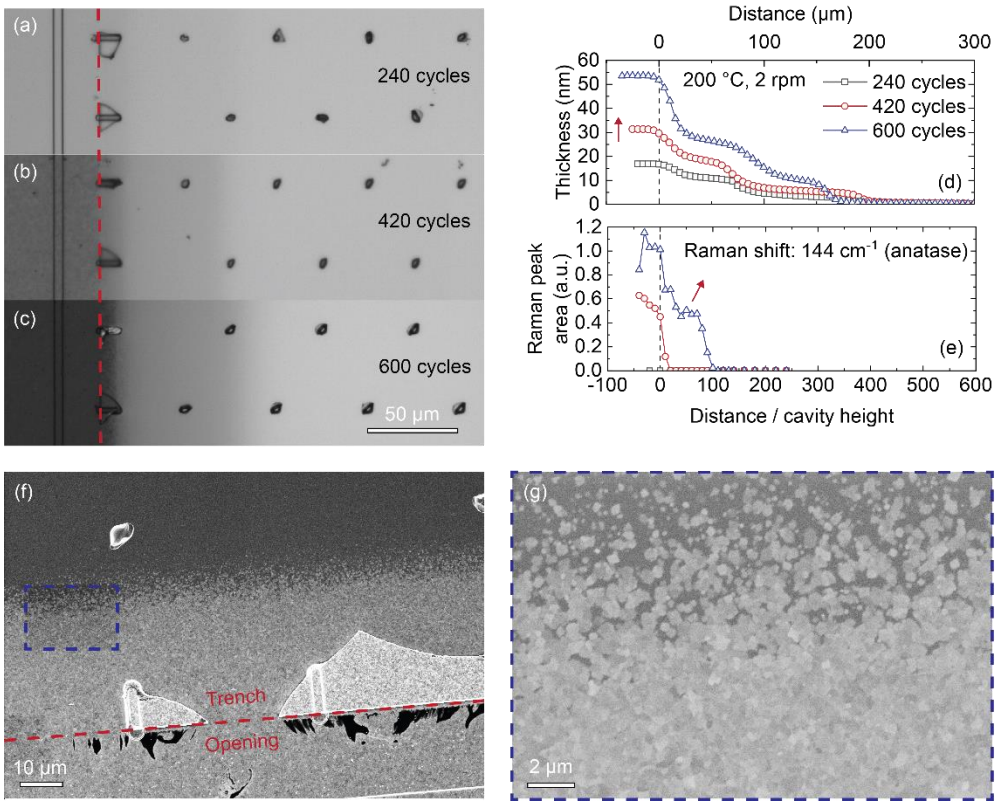

Figure 3: While TiO_2 films deposited in LHAR structures have large penetration depth in the trenches, only part of the film is crystalline. As a result of the crystallinity, this part of the film has grown thicker. Optical microscopy images of (a) 240 cycles, (b) 420 cycles, and (c) 600 cycles TiO_2. (d) Film thickness, and (e) Raman peak area normalized to film thickness as function of distance in the structure. SEM image of (f) the start of the structure and (g) close-up of the transition from anatase to amorphous film.

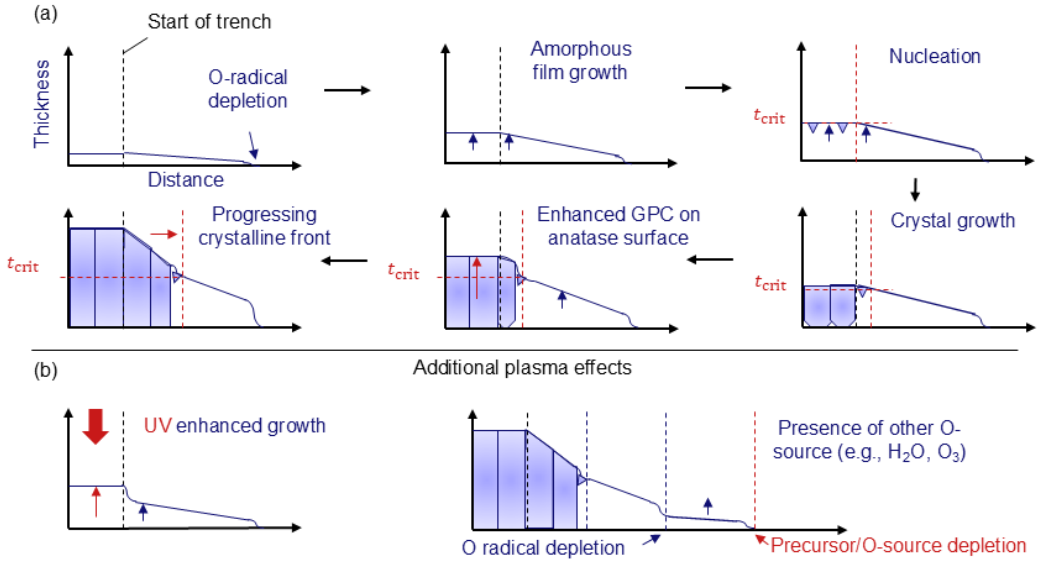

Figure 4: Schematic depiction of the influence of crystallization on conformality of TiO_2 ALD inside a LHAR structure. (a) Growth and crystallization mechanism. Black dashed line represents the start of the trench, red dashed horizontal and vertical lines represent the critical film thickness for nucleation, and the crystallization front inside the trench, respectively. (b) Additional effects that occur in the case of PE-s-ALD. Note that thickness is typically in the nm range, while distance is typically in the µm range.